Determination of Protein-Bound Palmitate Turnover Rates Using a Three-Compartment Model That Formally Incorporates [^{3}H]Palmitate Recycling†

Riad Qanbar‡ and Michel Bouvier*,‡,§

Department of Biochemistry and Groupe de Recherche sur le Système Nerveux Autonome, Université de Montréal, Montréal, QC, Canada H3C 3J7

Received April 23, 2004; Revised Manuscript Received July 20, 2004

ABSTRACT: The observation that the palmitoylation state of certain proteins can be biologically modulated led to the proposal that it could, much like phosphorylation, be an important dynamic regulator of protein function. However, based on single-phase exponential decay analysis of data from [^{3}H]palmitate pulse/chase experiments, the measured protein-bound palmitate turnover rates were often found to be too slow to account for rapid physiological responses. This paper reports that exponential decay does not adequately describe the results of such experiments because it fails to account for the recycling of [^{3}H]palmitate from cellular lipids to palmitoyl CoA. Taking this recycling into account, a three-compartment model was used to deduce the time-dependent changes of cellular [^{3}H]palmitoyl CoA and to infer the time course for the incorporation of [^{3}H]palmitate into proteins. The validity of the inferences made by the model was checked against data obtained by metabolic labeling of endogenous HEK293 cell proteins. In addition, the model could account for reported anomalies, discrepancies, and apparently paradoxical observations obtained by traditional analysis of data from pulse/chase experiments. Including the recycling of cellular palmitate in the formal description of the system offers a new tool for quantitative assessment of protein-bound palmitate turnover rates. Through the re-evaluation of these rates, the model provides a means for the reassessment of the potential physiological implications of dynamic palmitoylation. The model may also be generally applicable to other areas of research where recycling of tracer is a concern.

Many cellular proteins are modified with lipids. Of these modifications, palmitoylation, the thioesterification of sulfhydryl groups on cysteine residues by palmitic acid, stands out as the one most amenable to dynamic regulation due to its reversible nature. In several instances, the dynamic palmitoylation of a protein has been shown to have important functional consequences. Changes in the palmitoylation state have been shown to influence the subcellular distribution of some proteins and to regulate their attachment to specific membrane domains (*1*, *2*). For integral membrane proteins, where palmitoylation is not required for membrane insertion, this lipid modification has been found to influence diverse functions, including protein−protein interactions (*3*, *4*) and phosphorylation (*5*−*8*).

The multiple regulatory roles proposed for palmitoylation led many investigators to study the dynamic nature of this reaction (*9*). In most cases, classical pulse/chase experiments were carried out under different experimental conditions. To estimate turnover rates, the resulting data were analyzed according to a single-phase exponential decay model. Although such studies yielded data establishing palmitoylation as a dynamic process that can be regulated by various stimuli (*10*−*13*), the absolute values obtained for the turnover rates of the protein-bound palmitate were often puzzling. In one extreme case, the α_{2A} adrenergic receptor, the half-life of the protein-bound palmitate was calculated to be longer than that of the carrier protein (*14*)—a scenario that is impossible. However, even when the protein-bound palmitate half-life was found to be shorter than that of the carrier protein, most measurements made in mammalian cells gave values that are too large for a modification involved in rapid physiological responses. This can be best illustrated by comparing the reported half-life values for palmitoylation [1−5 h (*15*−*18*)] to those observed for another dynamically regulated post-translational modification, phosphorylation [half-life can be of the order of seconds (*19*, *20*)].

This prompted researchers to seek alternative mathematical models to fit the data from pulse/chase experiments (*21*, *22*). For example, a two-phase exponential decay equation was used to estimate the turnover rate of H-Ras (*23*). This analysis broke the decay curve into two components, a fast one and a slower one. The faster component was then used to calculate the half-life of H-Ras in mammalian cells. However, no formal analysis of the biochemical basis for such biphasic behavior was elaborated.

Whether monophasic or biphasic models are applied, experimental data from palmitoylation pulse/chase experiments often deviate from the expected behavior for expo-

† This work was supported by a research grant from the Canadian Institutes for Health Research. M.B. is the Canada Research Chair in Signal Transduction and Molecular Pharmacology.

* Address correspondence to this author at the Department of Biochemistry, Université de Montréal, C.P. 6128 Succursale Centre-Ville, Montréal, PQ, Canada H3C 3J7 [telephone (514) 343-6372; fax (514) 343-2210; e-mail michel.bouvier@umontreal.ca].

‡ Department of Biochemistry.

§ Groupe de Recherche sur le Système Nerveux Autonome.

10.1021/bi049176u CCC: $27.50
Published on Web 08/28/2004

nential decay. For instance, instead of decreasing, the incorporation of radiolabeled palmitate into proteins often remains unchanged (*24*) or even continues to increase (*25*) for a considerable period of time after the beginning of the chase. This initial increase is so common that many protocols for palmitoylation experiments call for extensive and prolonged washing or a "pre-chase" period in which time is given for this increase to subside before using the rest of the data for exponential decay analysis (*21*).

The explanation most often used to account for the deviation of experimental data from an exponential decay model is that cells require time to charge palmitoyl CoA stores. In other words, the transport and conversion of [^{3}H]palmitate to [^{3}H]palmitoyl CoA require a period of time of the order of an hour, so that when extracellular palmitate is withdrawn, the effect of withdrawal on the intracellular palmitoyl CoA lags an hour or so behind. Although logical, this hypothesis has never been validated experimentally.

Taken together, the above considerations indicate that, currently, there is no validated model that adequately describes protein palmitoylation kinetics. This constitutes a major obstacle in studies aimed at dissecting the mechanisms involved in regulating the palmitoylation/depalmitoylation reaction cycle. The present study was therefore conducted to characterize the biochemical basis underlying the apparently paradoxical nature of data obtained from palmitoylation turnover studies. This characterization allowed us to propose an alternative model describing the dynamics of [^{3}H]palmitate labeling so that reliable quantitative assessment of protein-bound palmitate turnover rates can be obtained.

MATERIALS AND METHODS

Metabolic Labeling Experiments. HEK293 cells were grown in DMEM containing 10% FBS and 2 mM glutamine (complete DMEM) to 70−75% confluence in 6 × 35 mm plates. Unless otherwise specified, cells were incubated in serum-free DMEM for 1 h prior to labeling. Ethanol-containing [^{3}H]palmitate (43−60 Ci/mmol) was dried under a stream of nitrogen gas. The labeled palmitate was taken up in a volume of DMSO not exceeding 1% of the final volume of the labeling medium and then diluted with the desired volume of serum-free DMEM prewarmed to 37 °C. Serum starvation and the use of serum-free media for labeling were meant to maximize uptake, but the serum-starvation step can be omitted and serum can be included in the labeling media without major attenuation of palmitate uptake (Supporting Information Figure 1). Final label concentrations used were at 50−250 μCi/mL. Unless otherwise specified, the label was used at the specific activity of the commercial product. When different, the specific activity of the label was modified by using excess unlabeled palmitate. After the desired labeling period, the radioactive medium was removed and cells were either harvested or incubated in the chase medium of choice for the indicated time before harvesting. Chase media used for the experiments reported here were (1) serum-free DMEM, (2) complete DMEM, and (3) complete DMEM containing excess unlabeled palmitic acid (final concentration as indicated in figure legends). Whenever unlabeled palmitate was used, it was dissolved in DMSO and then diluted with the medium of choice (chase or labeling medium). In all cases, the final concentration of DMSO was ≤1%.

SDS−PAGE, Depalmitoylation, and Fluorography. Following labeling, the medium was removed and cells were washed with 1 mL of ice-cold Tris-buffered saline per well and lysed on ice for 10 min in 0.5 mL of 50 mM Tris, pH 8.0, containing 0.4% deoxycholate, 1% NP40, 62.5 mM EDTA, 5 mM *N*-ethylmaleimide, 2 μg/mL aprotinin, 5 μg/mL soybean trypsin inhibitor, 5 μg/mL PMSF, and 2 μg/mL leupeptin. Lysates were then centrifuged for 1 min at 4 °C to get rid of nuclei and cell debris. Supernatants were transferred to fresh tubes, and 10 μL of 10% SDS was added to each sample (final concentration of 0.2%). Aliquots, typically 10−20 μL, were added to an equivalent volume of 2× nonreducing Laemmli sample buffer (final concentration of 50 mM Tris, pH 6.8, containing 2% SDS, 15% glycerol, and 0.05% bromophenol Blue), heated at 95 °C for 3 min, and loaded on nonreducing 10% SDS−polyacrylamide gels for electrophoresis. Proteins were then transferred to PVDF membranes. The membranes were dipped in methanol, thoroughly dried, treated with EA-Wax (Interscience) for fluorography, and then exposed to Kodak Biomax MR film for a period ranging from 1 to 8 weeks.

Quantification of Fluorograms. Fluorograms were scanned using an Arcus II laser scanner and the scanning data captured using Agfa Fotolook 32 software (version 3.6). Densitometric quantification was performed using Bio-Rad Quantity One software (version 4.4.1). For each individual protein, the size of the quantified area was kept constant. The background was subtracted by using the "global" method, whereby the density of an unlabeled area of the same size as the ones being quantified and from the same fluorogram was subtracted from the density of the quantified bands. The linearity of detection was checked using different exposure times of the same gel. When data from multiple gels were compared, all were exposed simultaneously for the same period of time and on the same film. No case of overexposure was encountered for any of the data presented.

Monitoring the Course of Label Incorporation. Aliquots of the labeling media (5 μL) were collected at the times indicated in the figures to estimate label uptake into cells. After the cells were lysed, aliquots (5 μL) of lysates were also counted. Protein concentration in the lysates was determined using a modification of the method of Lowry (D_C kit from Bio-Rad). To quantify phospholipids in the samples, 100 μL of 4.5% KCl (final concentration of 1%) was added to 350 μL of the lysates. The samples were then extracted with 1 mL of chloroform/methanol (1:1, v/v) (*26*), and the chloroform phase was transferred to glass tubes for evaporation under a stream of nitrogen gas. After the samples were ashed in 0.5 mL of 70% perchloric acid, inorganic phosphorus was determined according to the method of Rouser et al. (*27*). Phosphorus values were used to approximate the amount of phospholipids in the samples.

Calculations. (a) [^{3}H]Palmitoyl CoA Pool Kinetics. We used a closed three-compartment system to represent the major palmitate-involving reactions (*28*, *29*) on a time scale where growth, oxidation, and de novo palmitate synthesis can be assumed to be negligible. It is also assumed that palmitate conversion into palmitoyl CoA occurs at a very rapid rate compared to uptake, so as to consider uptake the rate-limiting step (*29*). [^{3}H]Palmitate is taken up by the cells and into the palmitoyl CoA at a variable rate, $R(t)$. The palmitoyl CoA pool feeds into the recyclable palmitate pool

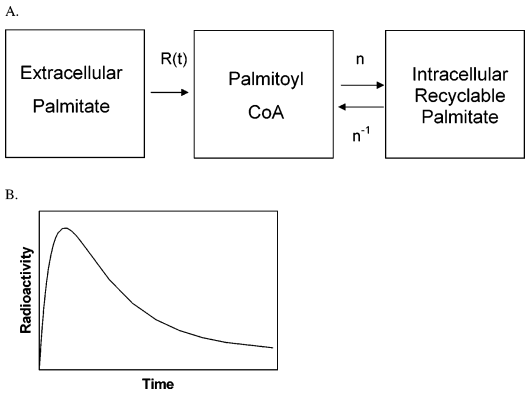

FIGURE 1: Modeling [^{3}H]palmitoyl CoA kinetics during the course of a [^{3}H]palmitate labeling experiment. (A) Schematic representation of the three-compartment model. Palmitate uptake into the cells occurs at a variable molar rate, $R(t)$, determined, in part, by the concentration of palmitate provided to the cells. Once inside the cells, activation of palmitate into palmitoyl CoA is assumed to be very rapid so as not to exert an effect on the mathematical approximation. Palmitoyl CoA feeds into a recyclable cellular palmitate pool (various cellular lipids that incorporate palmitate moieties and can release free palmitate as a result of lipid de-esterification) at a rate of n and is returned at a rate of n^{-1}. Growth, de novo fatty acid synthesis, and oxidation are assumed to be negligible over the duration of an experiment. (B) Graphic representation of the equation describing the changes in the intracellular [^{3}H]palmitoyl CoA pool during the course of a labeling experiment (eq 2 under Materials and Methods).

at a constant rate, n, and is returned from the recyclable palmitate pool to the palmitoyl CoA pool at a constant rate, n^{-1} (Figure 1). For a comprehensive description of compartments and mathematical tracer kinetics, the reader is referred to Sheppard (*30*).

In this simple three-compartment system, the changes in tracer amount within the palmitoyl CoA pool can be described by the differential equation

$$dS^*/dt = R(t) + W^*(t)/W_c \times n^{-1} - S^*(t)/S_c \times n \quad (1)$$

where $R(t)$ is the uptake rate of [^{3}H]palmitate at a given time, t; $S^*(t)$ and $W^*(t)$ are the amounts of tracer in the palmitoyl CoA and recyclable palmitate pools, respectively; and S_c and W_c are the total amounts of palmitoyl CoA and recyclable palmitate, respectively.

The uptake rate, $R(t)$, can be calculated on the basis of the kinetics of either label disappearance from the labeling medium or label association with the cells. Label disappearance from the medium can be accurately described by an exponential decay function:

$$I_{out}^*(t) = I_c^* \times e^{-mt} + I_{eq}^*$$

where $I_{out}^*(t)$ is the amount of radioactivity remaining in the medium at any time point, t; I_c^* is the maximum amount of radioactivity that can associate with the cells; m is the uptake constant (which can be used to calculate the half-life of label disappearance from the medium); and I_{eq}^* is the residual radioactivity remaining in the medium after extended labeling periods. The first derivative of this equation gives the negative of the rate of uptake, that is

$$R(t) = m \times I_c^* \times e^{-mt}$$

Alternatively, the amount of radioactivity that becomes associated with the cells at any point in time, $I_{in}^*(t)$, can be accurately described by an exponential association equation:

$$I_{in}^*(t) = I_c^* \times (1 - e^{-mt})$$

The first derivative of this equation describes the uptake rate, that is

$$R(t) = m \times I_c^* \times e^{-mt}$$

At any point in time, the total cell-associated radioactivity [i.e., $I_c^*(1 - e^{-mt})$] can be assumed to be the sum of the [^{3}H]palmitoyl CoA and recyclable [^{3}H]palmitate pools. Thus

$$W^*(t) = I_c^* \times (1 - e^{-mt}) - S^*(t)$$

Substituting for $W^*(t)$ in eq 1 and then solving the differential equation at the initial condition of $S^*(0) = 0$ yields

$$S^*(t) = F \times e^{-mt} + G - (F + G)\, e^{-ct} \quad (2)$$

where the new terms are defined as follows:

$$c = A + B \text{ (where } A = n^{-1}/W_c \text{ and } B = n/S_c)$$

$$F = I_c^* \times (m - A)/(c - m), \text{ and}$$

$$G = I_c^* \times A/c$$

The constant, c ($=A + B$), describes the turnover rate of palmitoyl CoA.

(b) Protein [^{3}H]Palmitoylation Kinetics. The palmitoylation reaction of any given protein can be chemically symbolized as

$$\text{palmitoyl CoA} + \text{protein} \underset{K^{-1}}{\overset{K}{\rightleftharpoons}} \text{palmitoylated protein} + \text{CoA}$$

Assuming the increase in protein and palmitoyl CoA pool sizes due to growth is negligible, the change in protein-associated radioactivity can be described by the differential equation

$$dP^*/dt = S^*(t)/S_c \times K - P^*(t)/P \times K^{-1} \quad (3)$$

where $P^*(t)$ is a function that describes the time course of [^{3}H]palmitate incorporation into a protein of interest; P is the total amount of palmitoylation sites on this particular protein (assumed to be equal to the molar protein amount); and K and K^{-1} are the rate constants for palmitoylation and depalmitoylation, respectively.

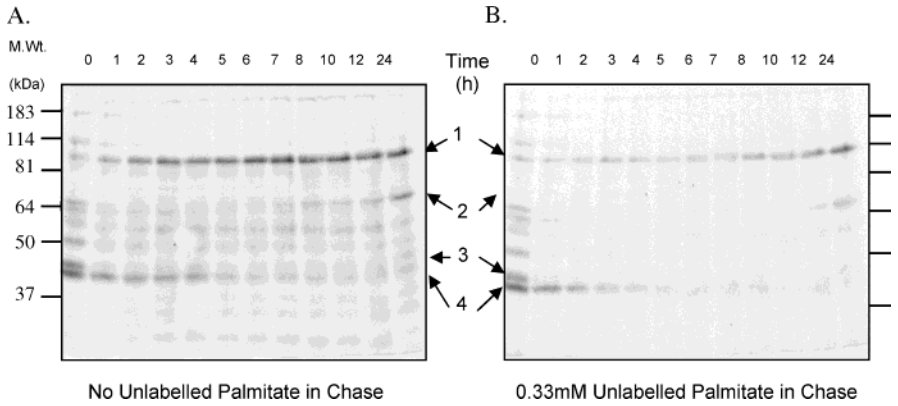

FIGURE 2: Pulse/chase labeling of endogenous HEK293 cell proteins as shown by fluorograms of SDS−PAGE resolving the lysates form cells, labeled for 15 min with [^{3}H]palmitate (200 μCi/ml, 60 Ci/mmol) and chased with either complete DMEM (A) or complete DMEM containing 0.33 mM palmitate (B). Numbers 1−4 refer to protein bands showing different labeling patterns. Results are representative of three experiments. Exposure was for 8 weeks.

The specific solution to eq 3 at the initial condition of $P^*(0) = 0$ is

$$P^*(t) = H \times e^{-mt} + J + L \times e^{-ct} - (H + J + L) \times e^{-kt} \quad (4)$$

where the new terms are defined as follows:

$$k = K^{-1}/P$$

$$H = K/S_c \times F/(k - m)$$

$$J = K/S_c \times G/k, \text{ and}$$

$$L = -K/S_c \times (F + G)/(k - c)$$

The constant, k, describes the palmitate turnover rate on the protein of interest.

Equation 4 is composed of three exponential terms and a constant. The unknowns defining the overall kinetics of the system, including the turnover rates for protein-bound palmitate and palmitoyl CoA, can thus be determined, in most cases, using the method of residuals, also known as exponent peeling. An explanation of this method can be found in most books dealing with pharmacokinetics (e.g., ref *31*) or with the use of tracers in biology (e.g., ref *32*). Alternatively, the data can be fitted to a user-defined equation using a suitable software package such as Prism (GraphPad Software). However, for meaningful estimations, many properly spaced data points are required over the ranges of the three rate constants (label uptake, m; palmitoyl CoA turnover, c; and protein-bound palmitate turnover, k). Calculating the uptake rate, m, by monitoring the radioactivity associating with the cells or remaining in the media can assist greatly in the assignment of the constants to the equation when exponent peeling is used. Even when computer-aided equation fitting is used, calculating m significantly increases the reliability of the analysis because it is necessary to keep the number of unknowns to a minimum. In most cases, fit results for eq 4 are unreliable if the number of unknowns exceeds three, so approximations and/or additional information obtained from exponent peeling can also greatly enhance computer-aided data fitting.

RESULTS

As indicated in the Introduction, several studies addressing palmitoylation kinetics using conventional pulse/chase experiments have led to results that raise serious doubts about the validity of the analysis traditionally applied to this type of approach. In an effort to more systematically characterize the apparent anomalies associated with the interpretation of the data, we followed commonly used protocols to conduct pulse/chase labeling experiments in HEK293. As per these protocols, we metabolically labeled the cells with [^{3}H]palmitate, replaced the label with fresh, tracer-free media to initiate the chase, and analyzed the incorporation of radioactivity into endogenous HEK293 proteins at various time points into the chase. We also assessed the effect of adding excess unlabeled palmitate to the chase media. This addition is usually made with the intent of ensuring that the specific activity of the tracer is reduced to insignificant levels inside the cells during the chase phase of the experiment.

A chase should result in an exponential reduction in the label associated with all proteins. As can be seen in Figure 2, this is clearly not the case either in the absence (A) or in the presence (B) of a 100-fold excess of unlabeled palmitate in the chase media. The incorporated radioactivity was hydroxylamine-sensitive, confirming the thioester nature of the linkage between the label and the protein (Supporting Information Figure 2). The incorporation of [^{3}H]palmitate into several proteins, as indicated by the intensity of the corresponding bands, continued to increase for hours after the withdrawal of the label. Examples of two such bands are pointed out in Figure 2 (bands 1 and 2). In one of these bands (band 2), a robust increase was seen even after 24 h of chase. Assuming the occurrence of an effective chase, such an increase can be explained in two ways. It could result from the processing of the protein, in which case the increase in intensity of label in a given band should be paralleled by a similar decrease in the labeling of another. Alternatively, it could result from a time lag required for palmitate uptake and its conversion into the active species in protein palmitoylation, palmitoyl CoA. Both possibilities can be easily ruled out when the pattern of [^{3}H]palmitate labeling of endogenous proteins is studied.

A precursor−product relationship between two bands would require that the total amount of detected label in the two forms not exceed at any given time point the corresponding amount at a previous time. It is evident from Figure 2 that the total label seen at 24 h exceeds the amounts detected at several earlier time points (5, 6, 7, and 8 h),

indicating that at the 24 h time point, the incorporated palmitate in bands 1 and 2 in Figure 2 could not have arisen from the processing of other bands.

A lag time in the actual commencement of chase would entail that label incorporation should increase in all labeled proteins for an identical period of time, followed by a universal decrease at different rates as the chase takes effect. As can be appreciated from Figure 3, where the time course of [^{3}H]palmitate incorporation into four different protein bands was plotted, no synchrony in labeling patterns exists. On the contrary, the label started decaying almost immediately in some bands (exemplified by bands 3 and 4 in Figure 3), whereas increases in labeling could still be detected in others many hours after the withdrawal of the label (exemplified by bands 1 and 2 in Figure 3).

With the two possibilities that could explain an increase in protein labeling in the course of a proper chase excluded, the initial premise of the occurrence of "chase" can be questioned. Indeed, an increase in the labeling of proteins during the "chase" can be readily explained by the persistence of significant amounts of tracer in the palmitoylation donor pool throughout the duration of the "chase" part of the experiment. This persistence could be a consequence of a palmitoyl CoA turnover rate that is slow enough to allow sufficient amounts of tracer to be incorporated into some proteins long after the start of the chase. When the rapid decay of most of the labeled proteins in Figure 3 is considered ($t_{1/2}$ of <30 min for protein band 3), it can be assumed that either the half-life of the removal of the [^{3}H]palmitoyl CoA from the palmitoyl CoA pool was at least that fast or that the labeled proteins were degraded rapidly. The latter possibility is unlikely for the following reasons: (1) the rapid decay in radioactivity was not peculiar to a specific protein band but was observed for most of the proteins that were labeled at the end of the pulse, and (2) the inclusion of excess unlabeled palmitate does change the absolute value of the incorporation, although not the appearance of the label incorporation curves (Figure 3), suggesting that the decrease in radioactivity is more likely to be related to the specific activity of the tracer than to the protein level. In addition, even though the half-life of palmitoyl CoA in HEK293 cells is not known, a rapid turnover would be more consistent with data in the literature because the half-life of palmitate in the palmitoyl CoA pool was reported to be ≤ 1 min in rat brain. To demonstrate the implication of palmitoyl CoA turnover for protein labeling, an upper limit of 30 min [based on the average half-life of label disappearance from the three most rapidly decaying proteins in the first hour of chase (<20 min)] was used to calculate the amount of radioactivity that remained in the palmitoyl CoA pool after 12 h. Because the total radioactivity associated with the cells at the end of the pulse was 30 μCi, the amount of [^{3}H]palmitoyl CoA left after 12 h (corresponding to 24 half-lives) at this removal rate would be <4 DPM, a value incompatible with the continued incorporation of detectable radioactivity in bands 1 and 2 (compare the labeling intensities at 12 and 24 h). Therefore, the persistence of the label leading to the protein labeling patterns seen in Figure 2 could not have resulted from a slow turnover rate of cellular palmitoyl CoA. To account for the observations, radiolabel must have been recycled into the palmitoyl CoA

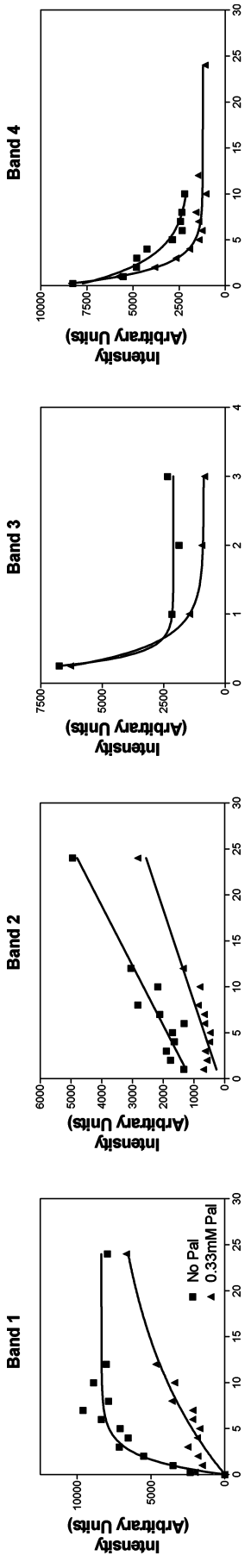

FIGURE 3: Time course of chase of [^{3}H]palmitate from the four endogenous HEK293 cell proteins identified in Figure 2. Labeling intensity was quantified in bands 1−4 using laser densitometry. The resulting values obtained in the presence (▲) and absence (■) of added palmitate in the chase medium were plotted against time and fitted to different equations [single-phase exponential association (band1), straight line (band 2), and single-phase exponential decay to a positive plateau value (bands 3 and 4)].

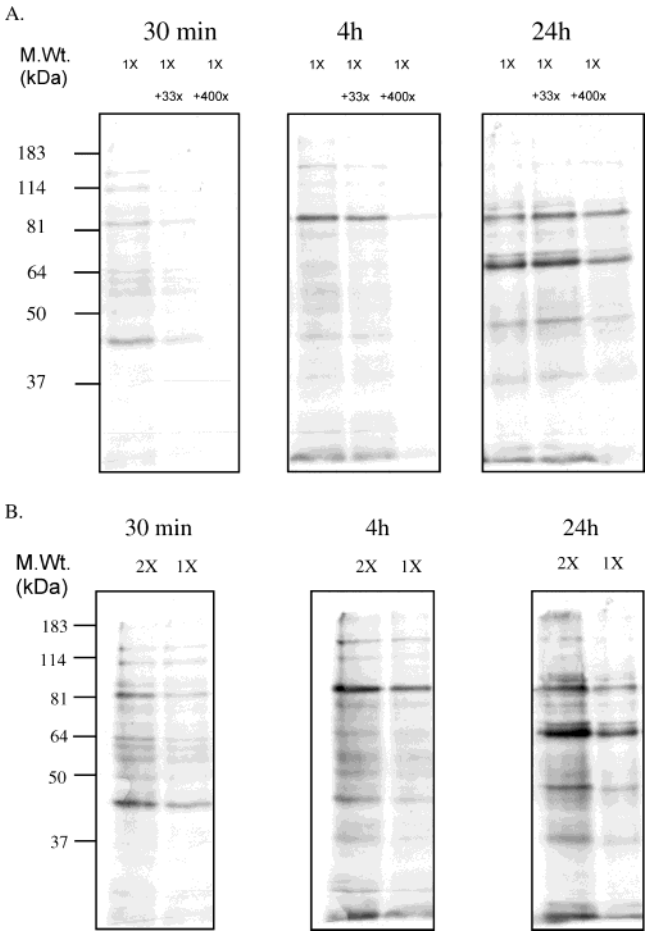

FIGURE 4: Influence of the absolute amount and specific activity of [^{3}H]palmitate on label incorporation into proteins as shown by fluorograms of SDS−PAGE resolving the lysates from cells labeled for the indicated times with [^{3}H]palmitate at the following amounts and specific activities: (A) 58 μCi/sample at 60 Ci/mmol (1*X*), 57.8 μCi/sample diluted 33 times with unlabeled palmitate to reach 1.75 Ci/mmol (1*X* + 33*x*), and 49.8 μCi/sample diluted 400 times with unlabeled palmitate to reach 0.15 Ci/mmol (1*X* + 400*x*); (B) 123.7 μCi/sample at 60 Ci/mmol (2*X*) and 58 μCi/sample at 60 Ci/mmol (1*X*). Results are representative of three experiments. Exposure was for 4 weeks.

pool, possibly through the hydrolysis of palmitate from intracellular sources that had already incorporated the label.

To test the possible occurrence of lipid recycling into the precursor pool, we pulse-labeled HEK293 cells using similar amounts of [^{3}H]palmitate at different specific activities. If no recycling of label took place, the specific activity of the label, after dilution with the intracellular pool, would be reflected in the labeling of proteins. This relative difference in labeling intensity among the different specific radioactivity samples should be independent of the time point at which the incorporation was assessed and thus should be maintained over the time course of the experiment. This was not the case. As Figure 4A illustrates, the relative label intensity of each band varied considerably according to the time at which the sample was collected. The substantial differences in protein labeling intensity observed at 30 min were attenuated by 4 h and almost completely gone by 24 h, indicating that at later time points only the total amount of radioactivity incorporated in the cell, and not its specific activity, determined the labeling intensity of the proteins. This point is further illustrated by contrasting the outcome of this

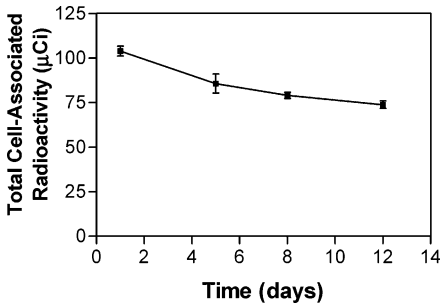

FIGURE 5: Time course of the loss of radioactivity associated with HEK293 cells. Following a 1 h labeling with [^{3}H]palmitate, cells were maintained in fresh media, and the radioactivity associated with the cells was measured at each passage for four passages. The graph shows the amount of radioactivity that remained associated with the cells after correction for the passage dilutions. The data shown are the means ± SEM of three experiments.

experiment with another where two different amounts of [^{3}H]palmitate at the same specific radioactivity were used to label the cells. In the latter case, as seen in Figure 4B, the relative amount of label was reflected in the protein labeling pattern throughout the duration of the experiment.

The only way by which these results could be explained in the absence of recycling is by assuming that the size of the intracellular palmitoyl CoA pool is too large to be significantly diluted by the addition of 330 nmol of palmitate and that accumulation of label continues to take place in the palmitoyl CoA pool throughout the duration of the experiment. Neither condition is consistent with the data. Indeed, in the experiment described in Figure 4A, the amount of palmitate taken up by the cells by 24 h reached ~300 nmol, an amount that is almost twice that of the largest palmitate pool in the cells, phospholipids, which we measured to be only 160 nmol. Furthermore, if radioactivity accumulated in the palmitoyl CoA pool throughout the duration of the experiment, a parallel accumulation of label into all labeled proteins would result. The individual labeling patterns of proteins in Figure 4 (panels A and B) unequivocally show protein-dependent variations, including nearly complete disappearance of radioactivity from some bands by 4 h. Taken together, these observations clearly suggest lipid recycling as the most likely explanation underlying the complex palmitate incorporation patterns observed in Figures 2 and 4. The hypothesis of lipid recycling is consistent with the observation that radioactivity remained associated with cells for extended periods of time following labeling. As shown in Figure 5, >50% of the [^{3}H]palmitate that was taken up remained associated with the cells after 12 days, mostly in the cellular lipid pool (data not shown).

The occurrence of lipid recycling could easily explain why classical exponential decay analysis of pulse/chase experiments often failed to provide reasonable estimates of protein-bound palmitate turnover. To offer an alternative solution, we elaborated a simple three-compartment model to describe the radioactivity in the palmitoyl CoA pool, taking into account the occurrence of palmitate recycling (Figure 1). In this model, the intracellular palmitoyl CoA pool is fed from two sources: an extracellular one originally providing the label and an intracellular source recycling it from the lipids back into the palmitoyl CoA pool via de-esterification and activation. Extracellular [^{3}H]palmitate is taken up by the cells with a given uptake constant, *m*. Its conversion into palmitoyl

CoA is assumed to be rapid enough so that the uptake, and not the conversion, represents the rate-limiting step. The intracellular palmitoyl CoA pool is assumed to feed into various lipid pools at an overall rate of n and be fed by many lipid de-esterification reactions at an overall rate of n^{-1}. On the bais of these rates and the sizes of the different pools, it is possible to calculate the amount of tracer present in all three compartments (eq 2; Figure 1). With the behavior of the tracer in the palmitoyl CoA pool known (eq 2), label incorporation into proteins can be predicted by eq 4 that contains three exponential terms determined by the [^{3}H]palmitate uptake constant, m, the palmitoyl CoA turnover rate, c, and the protein-bound palmitate turnover rate, k. (See Materials and Methods for the derivation of the equations.)

The change of experimental context from "chase" to "continuous labeling" carries a concomitant change in what variables need to be controlled and what constitutes a problem for the mathematical description. When a chase is performed, it is important to take into account the degradation of the labeled protein and the potential introduction of newly labeled protein to the system as a result of protein synthesis. In essence, the pulse/chase experiment is akin to looking at an elimination process (the disappearance of radioactivity), such as the removal of a metabolite from the blood stream. This is very different from what is under consideration in continuous labeling. Continuous labeling uses the changes in specific radioactivity (isotope dilution) and isotope distribution to infer the steady state of the system under study. Thus, provided that the system is at a steady state, continuous labeling provides a means of measuring protein-bound palmitate turnover without having to take protein synthesis or degradation into account.

Figure 6A describes the general shape of the protein palmitoylation curve predicted by the equation that describes the incorporation of radioactivity into a given protein in the course of a continuous [^{3}H]palmitate metabolic labeling experiment (eq 4). The model predicts an initial increase in tracer incorporation, which reaches a peak before it starts to decay. Clear of the peak region, the decay occurs exponentially, but it tapers off to a constant positive value (not to zero) that is reached once the specific activities of all the intracellular palmitate pools have equilibrated through the recycling processes.

The three-compartment-model-derived equation was then used to model the influence of the intrinsic protein-bound turnover rate of a given protein on its [^{3}H]palmitate incorporation curve. Figure 6B shows that decreasing the protein-bound palmitate turnover rate results in a rightward shift of the label incorporation peak and a decrease in its height without changing the overall shape of the curve. Interestingly, if tracer incorporation during a defined time period, delineated by arrows in Figure 6B, is plotted, the theoretical proteins with k values of 40, 0.4, and 0.004 yield labeling curves that can be fitted to different equations (Figure 6C), which are reminiscent of those obtained for endogenous HEK293 proteins reported in Figure 3 (compare the top panel of Figure 6C to Figure 3, band 1; the middle panel of Figure 6C to Figure 3, band 2; and the bottom panel of Figure 6C to Figure 3, bands 3 and 4). When a protein with a slow palmitate turnover such as protein band 2 in Figure 2 is considered, [^{3}H]palmitate incorporation into the protein will significantly lag behind the incorporation of

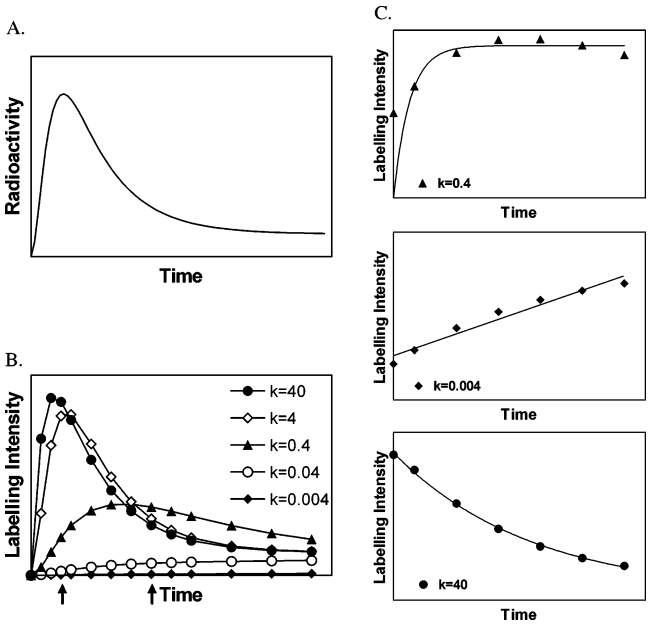

FIGURE 6: Simulations of [^{3}H]palmitate incorporation into proteins as a function of protein-bound palmitate turnover rates: (A) graphic representation of the equation describing label incorporation into proteins (eq 4 under Materials and Methods); (B) simulation of the effect of changing the palmitate turnover rate, k, on the time-dependent incorporation of [^{3}H]palmitate into proteins while keeping all other variables constant; (C) mathematical fits of the simulation data corresponding to the portions of the graphs delineated by the two arrows on the time coordinate of (B). The curves obtained for different k values were fitted to distinct equations (a single-phase exponential association for $k = 0.4$, a linear equation for $k = 0.004$, and a single-phase exponential decay equation for $k = 40$) closely resembling the experimental data obtained for different proteins in the pulse/chase experiment presented in Figure 3.

[^{3}H]palmitate into the palmitoyl CoA pool described in Figure 1B. At earlier times (when the specific activity of [^{3}H]palmitoyl CoA is at its peak), little [^{3}H]palmitate will be incorporated into the protein. However, the persistence of label in the palmitoyl CoA pool (due to plamitate recycling) despite the rapid turnover of the lipid will result in the accumulation of the protein-bound label over time. For a protein with rapid palmitate turnover (such as band 3 in Figure 2), the labeling of the protein will closely follow the labeling of palmitoyl CoA (Figure 1B). Thus, the protein-bound radioactivity will rapidly increase before decaying to an equilibrium value dictated by the total amount of radioactivity taken up by the cells and achieved via palmitate recycling.

The fact that the modeling of a continuous labeling experiment can adequately mimic some of the apparent anomalies of a pulse/chase experiment is not surprising because the recycling model predicts that the withdrawal of the label does not alter the shape of the curve. It merely changes its starting point and the values of the constants in the equations. However, it is important to note that data from pulse/chase experiments are not suitable for analysis by eq 4. Once the radioactivity is withdrawn from the media, the continuity of the processes that eq 4 describes is disrupted. The constants in the equation assume new values from the point of the start of the "chase". The new values for these constants are not readily available, calculable, or deducible,

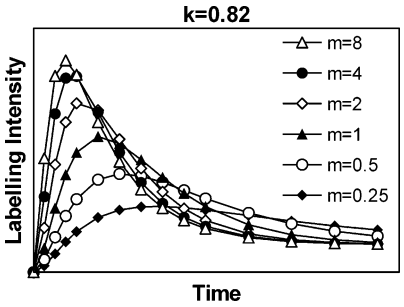

FIGURE 7: Simulations of [^{3}H]palmitate incorporation into proteins as a function of [^{3}H]palmitate uptake constant. The graph depicts the effect of changing the palmitate uptake constant, *m*, on the time-dependent incorporation of [^{3}H]palmitate into proteins, when all other variables were kept constant.

making any attempted analysis based only on the labeling data practically impossible.

In addition to accounting for previously inexplicable results, the model should permit the making of experimentally verifiable predictions. One of the predictions is that changes in experimental conditions that would lead to a decrease in the [^{3}H]palmitate uptake constant should shift the position of the labeling peak to the right and decrease its height (Figure 7). The validity of this prediction was tested by conducting a labeling experiment in which the [^{3}H]palmitate uptake constant was varied by changing the total amount of palmitate in the labeling media either by doubling the concentration of [^{3}H]palmitate (2*X*) or diluting the specific activity of the tracer by adding a 33-fold excess of unlabeled palmitate ($1X + 33x$). Uptake kinetics were then determined by measuring either the radioactivity remaining in the labeling media or that associated with the cells. As can be seen in Figure 8, the estimated uptake constants were similar in both cases, and as expected for a saturable process, increasing the total amount of palmitate reduced tracer uptake. The influence of this change in uptake rate on the actual labeling of endogenous HEK293 cell proteins is shown in Figure 9. As can be appreciated from the figure, changing the total amount of palmitate used in the labeling experiment affected the palmitoylation patterns substantially. Quantification of the [^{3}H]palmitate incorporation into three proteins is shown in Figure 10A. As predicted from the modeling (Figure 7), reducing [^{3}H]palmitate uptake by increasing the total label concentration (2*X*) or diluting the specific activity of the tracer with unlabeled palmitate ($1X + 33x$) resulted in changes in the position and magnitude of peak labeling that are most evident for proteins 2 and 3. Figure 10A also clearly shows that different proteins display very distinct palmitate incorporation kinetics. To determine if such differences could be accounted for by our model, we changed both the [^{3}H]palmitate uptake constant, *m*, and the protein-bound palmitoylation rate, *k*, in simulations using the three-compartment-model-derived equation. As shown in Figure 10B, modeling was done for three different theoretical proteins having distinct *k* values ($k1$, $k2$, and $k3$). For each theoretical protein, the same three uptake constants ($m1$, $m2$, and $m3$) were considered so as to mimic the type of experiment described in Figure 9. As can be appreciated, the modeled curves (Figure 10B) approximate reasonably well the experimental curves (Figure 10A). This is particularly evident for the protein corresponding to band 3.

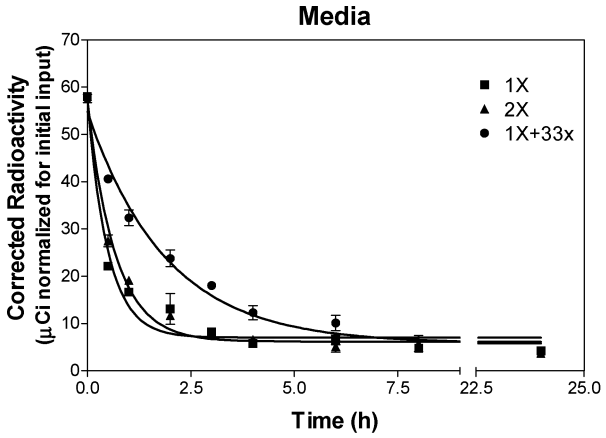

	1X	2X	1X+33x
HalfLife	0.3427	0.4646	1.319

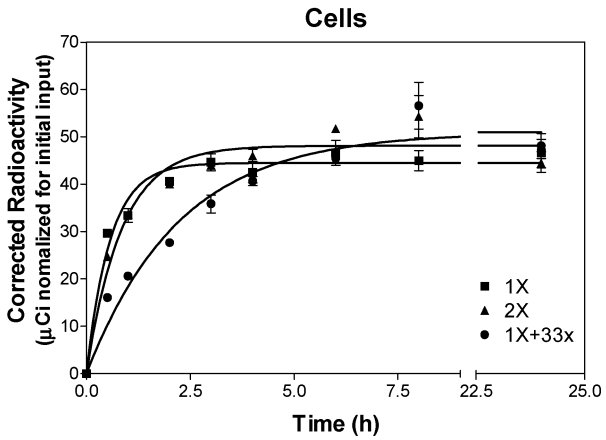

	1X	2X	1X+33x
HalfLife	0.3931	0.5850	1.549

FIGURE 8: HEK293 cell uptake of [^{3}H]palmitate under different conditions as assessed by measuring the radioactivity remaining in the media (A**)** or associated with the cells **(**B**)**, following labeling with [^{3}H]palmitate at the following amounts and specific activity values: (■) 58 μCi/sample at 60 Ci/mmol (1*X*), (▲) 123.7 μCi/sample at 60 Ci/mmol (2*X*), (●) 57.8 μCi/sample diluted 33 times with unlabeled palmitate to reach 1.75 Ci/mmol ($1X + 33x$). The 2*X* data were normalized to an input radioactivity of 58 μCi/sample by multiplying by 58/123.7 to facilitate visual comparison. The half-life values in each case were not affected by normalization and are given in tabular form at the bottom of the graph. The data in the graphs are presented as the means ± SEM of three experiments.

In addition to limitations of the detection and quantification techniques, the slight deviation of the experimental curves from the theoretical predictions can probably be explained in part by parameter changes that were not taken into account by our model. For instance, the hypotheses on the basis of which the model was developed call for negligible changes in the sizes of protein and lipid pools in the cells, limiting the time window during which samples can be collected for valid analysis. Under the experimental conditions used in the present study, this assumption was upheld reasonably well for at least the first 8 h. As can be seen in Figure 11A, no appreciable global change in protein content could be detected within that time. The absence of fluctuation in protein level for the individual proteins was also validated using polyacrylamide gel electrophoresis (see Supporting Information Figure 3). However, in the 24 h time frame considered for the experiments described in Figure 9, the

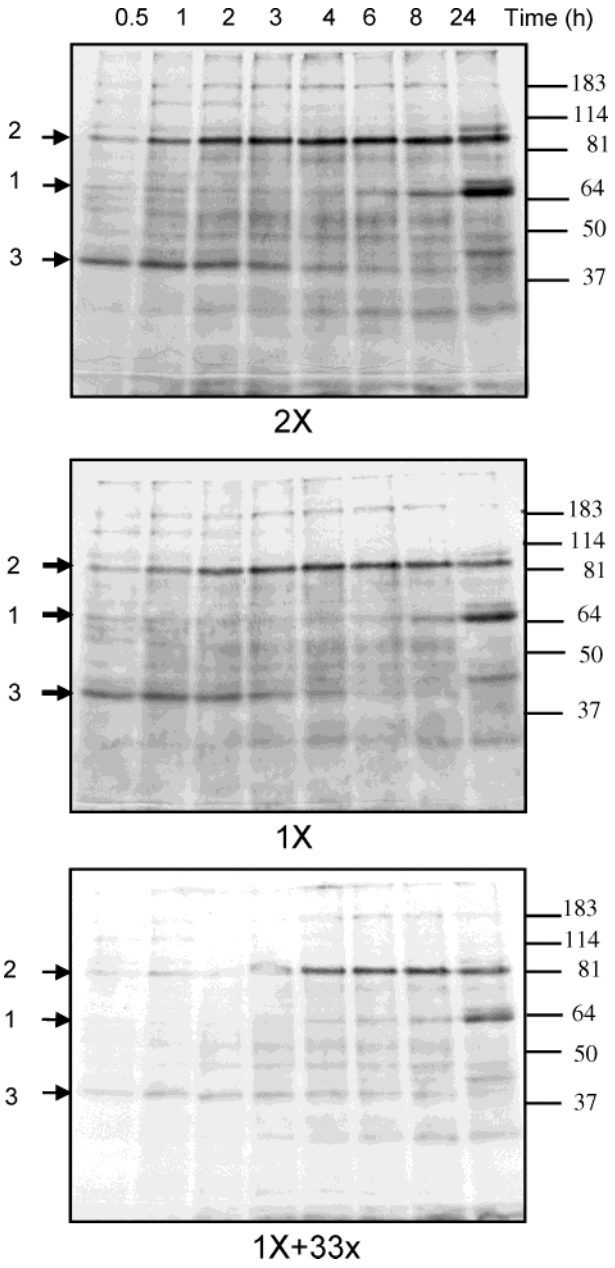

FIGURE 9: Effects of [^{3}H]palmitate uptake rates on label incorporation into proteins as shown by fluorograms of SDS−PAGE resolving the lysates from cells labeled with [^{3}H]palmitate at the following amounts and specific activities: 58 μCi/sample at 60 Ci/mmol (1*X*), 123.7 μCi/sample at 60 Ci/mmol (2*X*), and 57.8 μCi/sample diluted to 1.75 Ci/mmol with 33-fold unlabeled palmitate (1*X* + 33*x*). The arrows point to three protein bands (identified as 1−3), the labeling of which was further analyzed. Exposure was for 4 weeks. Results are representative of three experiments.

assumption that the growth-related increase in protein was negligible was not entirely upheld. In fact, both proteins (Figure 11A) and phospholipids (Figure 11B) had significantly increased by 24 h, indicating considerable cell growth. Moreover, the experimental changes in the uptake constant *m* were achieved by increasing the amount of palmitate added to the cells. As seen in Figure 11, such a change in culture conditions of the labeling experiment affected total protein and phospholipid synthesis differently, resulting in an increased phospholipid/protein ratio (Figure 11C). The trend toward an increase in phospholipid synthesis seen in Figure 11B suggests that the presence of excess unlabeled palmitate triggered a positive feedback loop in the phospholipid synthetic pathways and possibly activated other metabolic pathways (such as the β-oxidation pathway responsible for the utilization of fatty acids for energy production). Such a change in metabolism could conceivably influence protein palmitoylation kinetics. Therefore, it is advisable not to routinely include excess unlabeled palmitate in the labeling media when the objective of the experiments is to study the turnover of protein-bound palmitate under normal growth conditions.

Despite these limitations, the equation could fit the experimental data quite closely and thus could allow the calculation of palmitoylation rates using [^{3}H]palmitate uptake and protein-labeling data. However, this is only possible when the data points acquired during the experiment are sufficient to define the entire curve. Accordingly, we used the experimental data for band 3 in Figure 9 to estimate the half-life of protein-bound palmitate on that protein using exponent peeling and the triple-exponential equation (eq 4 under Materials and Methods). The values of the estimated protein-bound palmitate turnover rate were found to be similar, independent of the apparently different curves obtained in the three different labeling conditions when either the specific activity of the tracer or its amount was changed (Table 1). This clearly indicates that our proposed model can be confidently used to make a reliable assessment of palmitoylation kinetics under various experimental conditions.

Single-phase exponential decay analysis often used in previous studies to calculate palmitoylation turnover rates based on data from pulse/chase experiments ignores the contribution of palmitate recycling and the effect of the persistence of label in the palmitoyl CoA pool on the labeling of proteins. In fact, in its numerical consequences, it is akin to analyzing only the exponential decay portion of labeling curves presented in Figures 6−8 and 10 and assuming that exponential decay continues even in the plateau region of these curves. Such disregard for the plateau phase leads to gross overestimation of the decay constant. Moreover, even when the presence of a plateau is taken into account, single-exponential decay analysis allows the determination of only the slowest constant defining the curve. The slowest constant in the equations describing pulse/chase (not elaborated in this work) or continuous labeling (eq 4) experiments is not necessarily the turnover of protein-bound palmitate. The assertion that only the slowest component defining the system dictates the exponential decay portion of the curve was illustrated for continuous labeling experiments using theoretical examples derived from the curves in Figure 7, where label incorporation was simulated under different [^{3}H]palmitate uptake conditions (different *m* values) but a constant protein-bound palmitate turnover constant (*k*). As depicted in Figure 12, when only the exponential decay portion of the curves was considered, the decay constant was found to be indeed equal to *k* when *k* was smaller than *m*. However, when *m* was smaller than *k*, this decay constant became equal to *m*. This is to say that if the uptake was slower than protein-bound palmitate turnover, the analysis of the exponential decay portion of the curve would yield the uptake constant and not the palmitate turnover constant and vice-versa. This prediction is consistent with the analysis of the experimental data extracted from Figure 10A. Indeed, in the case of the

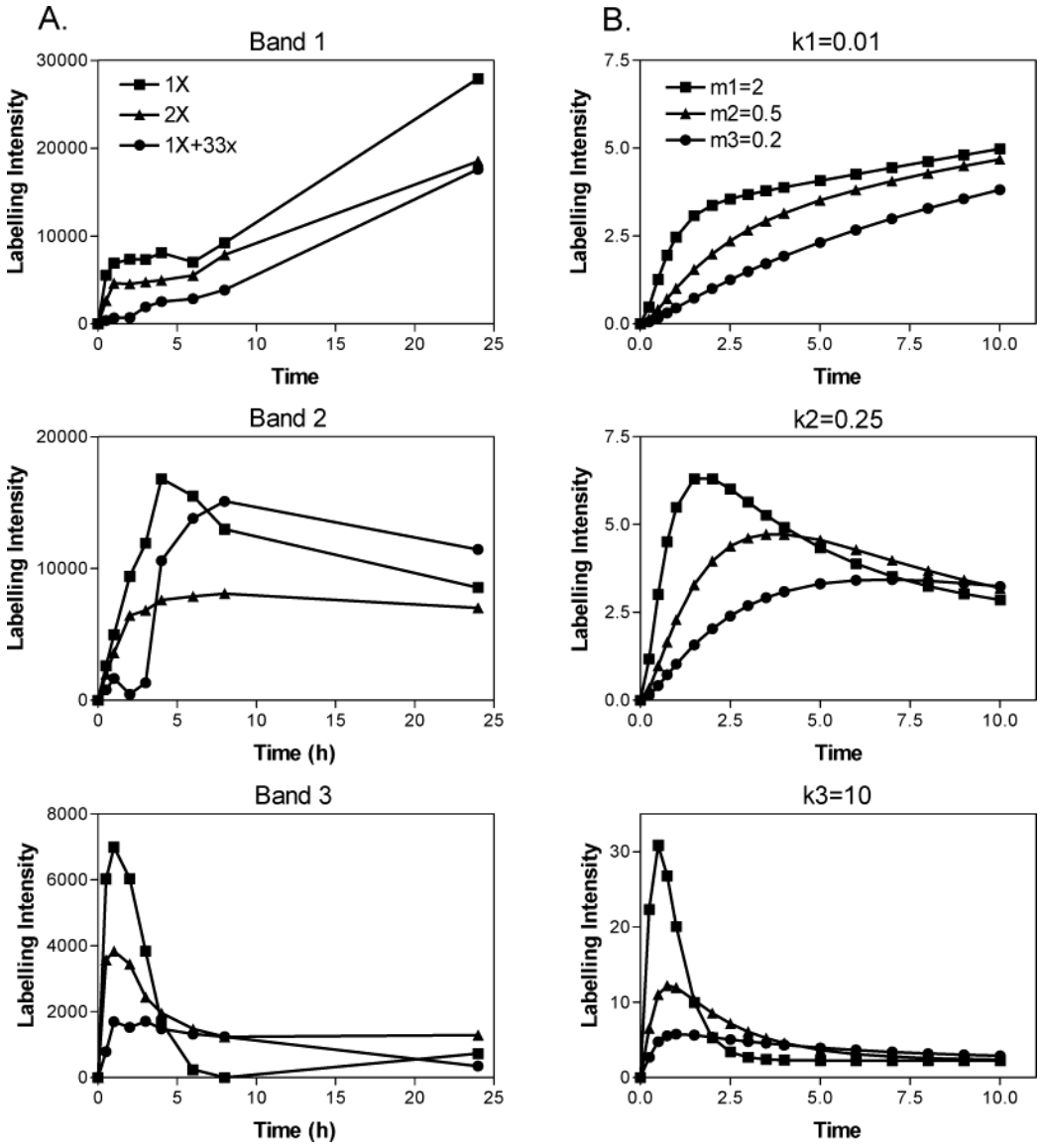

FIGURE 10: Comparison between metabolic labeling data and simulation results. (A) Graphic representation of the time-dependent change in the intensity of labeling for protein bands 1−3 in Figure 9. Quantification was performed using laser densitometry. To facilitate visual comparison, numbers were normalized to account for the different radioactivity input by multiplying the 2*X* values by 58/123.7. (B) Simulations of the labeling kinetics using eq 4. For each protein-bound palmitate turnover rate, *k*, three uptake constant values (*m*1, *m*2, and *m*3) were used. The same three *m* values were used to simulate the labeling kinetics of theoretical proteins with distinct protein-bound palmitate turnover rates (*k*1, *k*2, and *k*3).

protein band considered (band 3), the *k* values determined in all of the experimental conditions used were smaller than or similar to the experimentally determined uptake constant, *m*, so that the calculated decay rates based on the single-exponential decay portion of these curves were almost identical to those obtained using the triple-exponential eq 4 (Table 1).

DISCUSSION

The model developed in this work takes into account the contribution of [^{3}H]palmitate recycling to the specific radioactivity of the intracellular [^{3}H]palmitoyl CoA pool and thus its contribution to protein labeling in metabolic labeling experiments. Even though lipid recycling is a well-established fact (for review, see ref *28*), its relevance to protein palmitoylation was not elucidated until more recently. In a 1998 report, Tetzloff and Bizzozero (*33*) elegantly demonstrated the contribution of palmitate derived from lipid deesterification to protein palmitoylation. They incubated rat brain white matter slices with water containing ^{18}O, a stable oxygen isotope, and showed that it was possible to detect this isotope in the proteolipid protein, the major palmitoylated protein in these cells. The process entailed the hydrolysis of fatty acids from cellular lipids resulting in the appearance of ^{18}O in free palmitate that could be reactivated to ^{18}O-containing palmitoyl CoA and used to palmitoylate proteins. Yet, despite this clear demonstration of palmitate recycling into proteins, its implications for the kinetics of protein labeling with [^{3}H]palmitate remained largely ignored.

To take palmtiate recycling into account using the method presented in this paper, protein palmitoylation is monitored in [^{3}H]palmitate continuous metabolic labeling experiments. In addition to measuring the incorporation of labeled palmitate into proteins over a time range that allows the complete description of the labeling curve, the uptake of [^{3}H]palmitate also needs to be assessed by measuring either

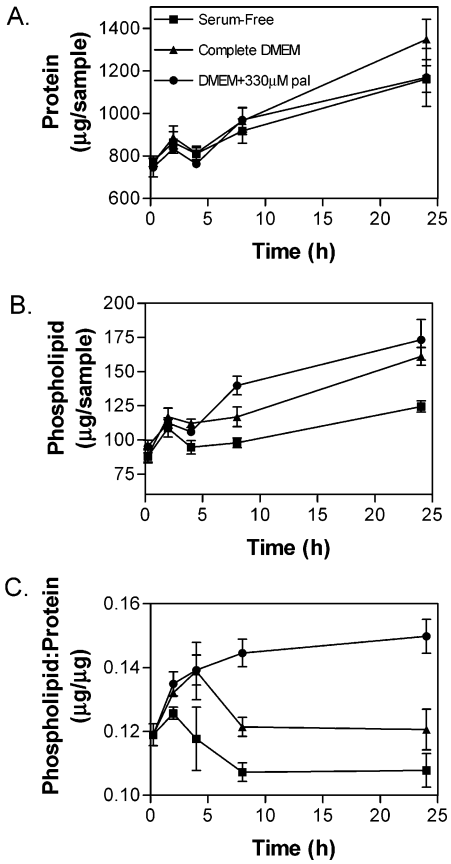

FIGURE 11: Time course for cellular growth under different radiolabeling conditions. HEK293 cells were either continuously labeled with [^{3}H]palmitate in serum-free DMEM (■) or labeled for 15 min and chased with either complete DMEM (▲) or DMEM containing 0.33 mM palmitate (●). Protein content (A), phospholipid content (B), and the ratio of phospholipid to protein (C) were estimated at the indicated times. The data are presented as the means ± SEM of six experiments.

Table 1: Calculation of the Apparent Rate Constant *k* for an Endogenous Protein in HEK293 Cells under Different Labeling Conditions

labeling conditions	m^a (h^{-1})	k^b (h^{-1})	$t_{1/2}{}^b$ (min)	k^c (h^{-1})	$t_{1/2}{}^c$ (min)
123.7 μCi at 60 μCi/nmol	1.492	0.5303	78	0.5315	78
58 μCi at 60 μCi/nmol	2.023	0.6298	66	0.5636	74
57.6 μCi at 1.75 μCi/nmol	0.5254	ND	ND	0.5311	78

[a] Calculated from the uptake of radioactivity from the media. [b] Calculated using exponent peeling. [c] Calculated using GraphPad Prism to fit the data to a user-defined equation.

its disappearance from the media or its appearance in the cells. The uptake constant, *m*, is required for solving the triple-exponential equation describing the protein labeling curves so as to determine the protein-bound palmitate turnover, *k*. The labeling can be conducted in the presence or absence of serum. Indeed, the effect that serum inclusion has on the uptake rate (*m*) (see Supporting Information Figure 1) is taken into consideration in the calculation of the protein-bound palmitate turnover (*k*) because the former parameter is experimentally determined and included in the equation. However, serum starvation often results in changes in protein palmitoylation and therefore may not accurately reflect the kinetics of protein palmitoylatoin under normal cell growth conditions.

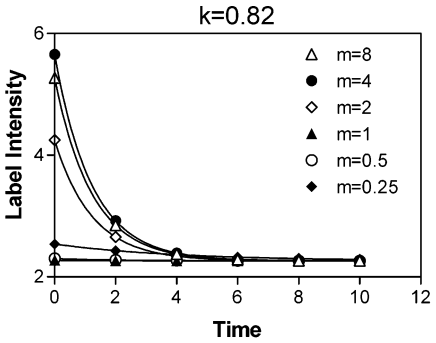

	m=8	m=4	m=2	m=1	m=0.5	m=0.25
K	0.8198	0.8193	0.8127	0.7987	0.4968	0.2498

FIGURE 12: Single-phase exponential decay portion of the simulation curves defined by the slowest component. The graph illustrates the results of fitting the exponential decay portions of the simulated curves in Figure 7 ($k = 0.82$ and *m* varying from 0.25 to 8) to a single-phase exponential equation (plateau not forced to 0). In each case, the apparent decay constant, *K*, was determined and is given in tabular form. Note that *K* is equal to the uptake constant, *m*, whenever *m* is smaller than the protein-bound palmitate turnover rate, *k*, and equal to *k* whenever *k* is smaller than *m*.

Once taken into account, the significance of the contribution of palmitate recycling becomes clear when the accuracy by which the new model describes experimental data is compared to that of the traditionally used exponential decay model. The elaborated model not only predicts the deviations of palmitoylation kinetics from traditional exponential decay behavior but also offers an explanation for paradoxical results and unrealistic half-life values sometimes obtained for protein-bound palmitate. As already indicated under Results, whereas exponential decay should result in a rapid decrease in protein-bound radioactivity upon withdrawal of label, an expectation hardly ever met by experimental data (e.g., refs *24* and *25*), the new model accommodates an initial slow decease or even an increase in radioactivity relative to a later time point.

Another deviation from the single-exponential decay model that is well accounted for by the recycling model is the tendency of protein-bound radioactivity not to decay to zero (e.g. ref *34*). This failure of protein-bound radioactivity to approach zero at a constant rate in pulse/chase experiments prompted researchers to try to fit the data empirically to other models, including a two-phase exponential decay model (*21*−*23*). The two-phase exponential decay model seemed to remedy two problems: that of the apparently slower decay at later times into the chase and that of the actual values of calculated half-lives, bringing them closer to a physiologically meaningful range. However, the biological factors underlying the two-phase exponential model used by the authors were not explicitly formulated within a mathematical description of the system. One of the reasons invoked to use such a double-exponential model was the possible contribution of multiple palmitoylation reactions on multiply palmitoylated proteins. However, careful analysis of the data ruled out this possibility (*21*). Recycling of [^{3}H]palmitate was also suggested as an explanation for the slower decay component in the two-phase model (*22*, *23*), but the mathematical implications were not formalized. In fact, as can be appreciated from the mathematical derivation presented under Materials and Methods, including the occurrence of recycling as a formal parameter in the description of the palmitoylation

kinetics led to an equation involving three exponential terms and not to a two-exponential decay curve.

Forcing single- or double-exponential decay analysis on the type of palmitoylation curves observed experimentally would be expected to lead to inaccurate estimation of the protein-bound palmitate turnover rates. In fact, a combination of the two factors discussed above, a slow decrease in disappearance of label at the beginning of an experiment and decay to an equilibrium value greater than zero, would lead to a significant overestimation of the palmitate half-life if an exponential decay analysis was forced to fit the data. A dramatic example of such overestimation is provided by a study on the α_{2A}-adrenergic receptor, where the half-life of the receptor-bound palmitate, as calculated using a simple exponential decay fit, was greater than the half-life of the carrier protein itself (*14*).

The complex [^{3}H]palmitoyl CoA kinetics described in the present study (Figure 1) has important implications for the design and interpretation of experiments investigating the dynamic regulation of protein palmitoylation. Changes in the specific activity of the palmitoyl CoA pool during the course of the experiments, whether in continuous labeling or pulse/chase experiments, would determine the direction of the protein palmitoylation changes observed upon application of specific stimuli. A stimulus that increases the palmitoylation turnover rate would lead to an increase in protein-labeling if its effect was monitored during the time in which the specific activity of the palmitoyl CoA pool was increasing (early time points). However, the same stimulus would result in a decrease in labeling if its effect was assessed during the phase in which the specific radioactivity of the palmitoyl CoA pool was decreasing (later time points). Not surprisingly, no change in [^{3}H]palmitate incorporation would be detected if the stimulus was applied once equilibrium had been reached. An example of such a phenomenon can be appreciated in studies describing the effect of agonist stimulation on the palmitoylation rate of the β_2-adrenegic receptor. Following an initial agonist-promoted increase in the [^{3}H]palmitate incorporation, the agonist treatment then led to a decrease in labeling when compared to nontreated cells (*34*, *35*).

The implications of these labeling kinetics are quite significant. If the effect of stimulation was studied at only one time point, the detected consequence of an increase in turnover can be an increase, a decrease, or no change in labeling intensity, depending on the position of the chosen time point relative to the peak of specific activity in the palmitoyl CoA pool. It follows that reports in the literature that may be contradictory at face value are reconcilable. For example, in the G-protein-coupled receptor family of proteins, agonist treatment produced an increase in receptor palmitoylation in some cases, little change in some, and a decrease in others (*9*).

The studies reported here also indicate that the experimental conditions can have significant effects on the observed palmitate turnover kinetics. For instance, adding excess palmitate to enhance the chase of tracer, as indicated in Figure 11, promotes an increase in phospholipid synthesis that alters the lipid/protein ratio in a way that may influence the palmitoylation of some proteins. To minimize the number of variables that need to be considered in any given experiment, we suggest the experiments be conducted in serum-supplemented media, in the absence of excess palmitate. In addition to reducing the number of variables in an experiment and maintaining steady-state kinetics, these modifications make the experiments technically simpler and maximize the signal.

The recycling model is essentially the sum of three exponential terms, with the constants in the exponents depending on the various rates (palmitate uptake, palmitoyl CoA turnover, and turnover of protein-bound palmitate; eq 4). The relative weight of each term in the equation critically depends on the value of each of the constants relative to the other two. This, in turn, determines whether, under certain conditions, a constant can be determined accurately, or even at all. For example, if the depalmitoylation of a protein (e^{-kt}) is much faster than both palmitate uptake (e^{-mt}) and palmitoyl CoA turnover (e^{-ct}), the value of the exponential term containing the protein depalmitoylation rate (e^{-kt}) becomes negligible compared to the other two. The implication of this fact is that if protein palmitoylation occurs at a very rapid rate, it will be impossible to measure. The range of rates included in this "rapid" category can be roughly outlined on the basis of published palmitoyl CoA turnover rates. Grange et al. (*29*) measured the half-life of the palmitoyl CoA pool in the brains of awake rats to be ≤ 1 min. Therefore, it is not unreasonable to conclude that when the half-life of protein-bound palmitate is <1 min, it will be difficult, or at times impossible, to measure. For proteins with slower palmitate turnover rates, the model should prove to be a useful tool to monitor protein palmitoylation dynamics.

The model allows the user to estimate the turnover rate, k, of palmitate on a protein and hence the half-life of the modification. However, because the actual depalmitoylation rate, K^{-1}, is linked to the protein concentration by the relationship $k = K^{-1}/P$, K^{-1} can be determined only if the total amount of the protein under study is known and the measurement is normalized to some parameter (e.g., unit total protein or unit total phospholipids). Another important implication of this relationship is that the experimentally determined turnover rate in a system where the protein under study is overexpressed is likely to be slower than the actual turnover rate under native expression levels. Consequently, although calculated turnover rates can provide very useful information concerning the dynamic nature of the palmitoylation of proteins, using them as absolute values in an effort to compare different proteins expressed in different systems, or even the same protein expressed at different levels, should be avoided.

It follows from the above discussion that accurate determination of dynamic changes in protein-bound palmitate turnover rate can be obtained only if the amount of the protein under study is not affected during the course of the experiments. This, however, should not be a concern in the case of rapid dynamic regulation accompanying events such as receptor activation, opening of a channel, or enzymatic activation because, in the time frame of such regulatory events, changes in protein concentration due to natural growth or induction of protein synthesis are unlikely to be significant. The fact that the measured protein-bound palmitate turnover rate is highly sensitive to the protein substrate concentration has another practical implication that should not be overlooked. The factor linking the protein content to

the palmitoylation rate is not the protein concentration per se but rather the number of available cysteines that can serve as substrate for the palmitoylation reaction. Therefore, the apparent half-life of protein-bound palmitate would also change with the total number of accessible palmitoylation sites on a specific protein. Consequently, stimuli that result in conformational changes, hiding or exposing cysteine residues, would lead to parallel changes in the measured half-life values.

Taking recycling into account and defining the effects of uptake rate and protein expression levels can be valuable in understanding the available literature on the dynamics of palmitoylation in a new light. In fact, palmitoylation may still prove to be a rapid-acting regulatory mechanism in studies that have previously suggested the reaction to be too slow for physiological significance. Even in studies where the turnover rates were found to be relatively fast, the actual values may turn out to be many times faster than initially thought. With revised turnover rates, palmitoylation can be viewed afresh in physiological context.

ACKNOWLEDGMENT

We thank Dr. Graciela Pineyro for helpful discussions and Dr. Monique Lagacé for comments on the manuscript.

SUPPORTING INFORMATION AVAILABLE

Figures displaying the uptake half-time of [^{3}H]palmitate, ^{3}H label associated with proteins in continuous metabolic labeling experiments, and cell lysates over the course of a continuous labeling experiment. This material is available free of charge via the Internet at http://pubs.acs.org.

REFERENCES

1. McCabe, J. B., and Berthiaume, L. G. (2001) N-terminal protein acylation confers localization to cholesterol, sphingolipid-enriched membranes but not to lipid rafts/caveolae, *Mol. Biol. Cell 12*, 3601−3617.
2. Yang, S., Zhang, L., and Huang, Y. (2001) Membrane association and conformational change of palmitoylated G(o)alpha, *FEBS Lett. 498*, 76−81.
3. O'Dowd, B. F., Hnatowich, M., Caron, M. G., Lefkowitz, R. J., and Bouvier, M. (1989) Palmitoylation of the human beta 2-adrenergic receptor. Mutation of Cys341 in the carboxyl tail leads to an uncoupled nonpalmitoylated form of the receptor, *J. Biol. Chem. 264*, 7564−7569.
4. Hayashi, M. K., and Haga, T. (1997) Palmitoylation of muscarinic acetylcholine receptor m2 subtypes: reduction in their ability to activate G proteins by mutation of a putative palmitoylation site, cysteine 457, in the carboxyl-terminal tail, *Arch. Biochem. Biophys. 340*, 376−382.
5. Moffett, S., Mouillac, B., Bonin, H., and Bouvier, M. (1993) Altered phosphorylation and desensitization patterns of a human beta 2-adrenergic receptor lacking the palmitoylated Cys341, *EMBO J. 12*, 349−356.
6. Palmer, T. M., and Stiles, G. L. (2000) Identification of threonine residues controlling the agonist-dependent phosphorylation and desensitization of the rat A(3) adenosine receptor, *Mol. Pharmacol. 57*, 539−545.
7. Hawtin, S. R., Tobin, A. B., Patel, S., and Wheatley, M. (2001) Palmitoylation of the vasopressin V1a receptor reveals different conformational requirements for signaling, agonist-induced receptor phosphorylation, and sequestration, *J. Biol. Chem. 276*, 38139−38146.
8. Kraft, K., Olbrich, H., Majoul, I., Mack, M., Proudfoot, A., and Oppermann, M. (2001) Characterization of sequence determinants within the carboxyl-terminal domain of chemokine receptor CCR5 that regulate signaling and receptor internalization, *J. Biol. Chem. 276*, 34408−34418.
9. Qanbar, R., and Bouvier, M. (2003) Role of palmitoylation/depalmitoylation reactions in G-protein-coupled receptor function, *Pharmacol. Ther. 97*, 1−33.
10. James, G., and Olson, E. N. (1989) Identification of a novel fatty acylated protein that partitions between the plasma membrane and cytosol and is deacylated in response to serum and growth factor stimulation, *J. Biol. Chem. 264*, 20998−21006.
11. Moffett, S., Adam, L., Bonin, H., Loisel, T. P., Bouvier, M., and Mouillac, B. (1996) Palmitoylated cysteine 341 modulates phosphorylation of the beta2-adrenergic receptor by the cAMP-dependent protein kinase, *J. Biol. Chem. 271*, 21490−21497.
12. Patterson, S. I. (2002) Posttranslational protein S-palmitoylation and the compartmentalization of signaling molecules in neurons, *Biol. Res. 35*, 139−150.
13. Bijlmakers, M. J., and Marsh, M. (2003) The on−off story of protein palmitoylation, *Trends Cell Biol. 13*, 32−42.
14. Kennedy, M. E., and Limbird, L. E. (1994) Palmitoylation of the alpha 2A-adrenergic receptor. Analysis of the sequence requirements for and the dynamic properties of alpha 2A-adrenergic receptor palmitoylation, *J. Biol. Chem. 269*, 31915−31922.
15. Baker, L. P., and Storm, D. R. (1997) Dynamic palmitoylation of neuromodulin (GAP-43) in cultured rat cerebellar neurons and mouse N1E-115 cells, *Neurosci. Lett. 234*, 156−160.
16. Lane, S. R., and Liu, Y. (1997) Characterization of the palmitoylation domain of SNAP-25, *J. Neurochem. 69*, 1864−1869.
17. Wolven, A., Okamura, H., Rosenblatt, Y., and Resh, M. D. (1997) Palmitoylation of p59fyn is reversible and sufficient for plasma membrane association, *Mol. Biol. Cell 8*, 1159−1173.
18. van de Loo, J. W., Teuchert, M., Pauli, I., Plets, E., Van de Ven, W. J., and Creemers, J. W. (2000) Dynamic palmitoylation of lymphoma proprotein convertase prolongs its half-life, but is not essential for trans-Golgi network localization, *Biochem. J. 352* (Part 3), 827−833.
19. Mao, S. Y., and Metzger, H. (1997) Characterization of protein-tyrosine phosphatases that dephosphorylate the high affinity IgE receptor, *J. Biol. Chem. 272*, 14067−14073.
20. Goldstein, B., Faeder, J. R., Hlavacek, W. S., Blinov, M. L., Redondo, A., and Wofsy, C. (2002) Modeling the early signaling events mediated by FcepsilonRI, *Mol. Immunol. 38*, 1213−1219.
21. Lu, J. Y., and Hofmann, S. L. (1995) Depalmitoylation of CAAX motif proteins. Protein structural determinants of palmitate turnover rate, *J. Biol. Chem. 270*, 7251−7256.
22. Baker, T. L., Booden, M. A., and Buss, J. E. (2000) S-Nitrosocysteine increases palmitate turnover on Ha-Ras in NIH 3T3 cells, *J. Biol. Chem. 275*, 22037−22047.
23. Baker, T. L., Zheng, H., Walker, J., Coloff, J. L., and Buss, J. E. (2003) Distinct rates of palmitate turnover on membrane-bound cellular and oncogenic H-ras, *J. Biol. Chem. 278*, 19292−19300.
24. Ponimaskin, E. G., Schmidt, M. F., Heine, M., Bickmeyer, U., and Richter, D. W. (2001) 5-Hydroxytryptamine 4(a) receptor expressed in Sf9 cells is palmitoylated in an agonist-dependent manner, *Biochem. J. 353*, 627−634.
25. Duncan, J. A., and Gilman, A. G. (2002) Characterization of *Saccharomyces cerevisiae* acyl-protein thioesterase 1, the enzyme responsible for G protein alpha subunit deacylation in vivo, *J. Biol. Chem. 277*, 31740−31752.
26. Bligh, E. G., and Dyer, W. J. (1959) A rapid method of total lipid extraction and purification, *Can. J. Med. Sci. 37*, 911−917.
27. Rouser, G., Fkeischer, S., and Yamamoto, A. (1970) Two-dimensional then layer chromatographic separation of polar lipids and determination of phospholipids by phosphorus analysis of spots, *Lipids 5*, 494−496.
28. Robinson, P. J., Noronha, J., DeGeorge, J. J., Freed, L. M., Nariai, T., and Rapoport, S. I. (1992) A quantitative method for measuring regional in vivo fatty-acid incorporation into and turnover within brain phospholipids: review and critical analysis, *Brain Res. Brain Res. Rev. 17*, 187−214.
29. Grange, E., Deutsch, J., Smith, Q. R., Chang, M., Rapoport, S. I., and Purdon, A. D. (1995) Specific activity of brain palmitoyl-CoA pool provides rates of incorporation of palmitate in brain phospholipids in awake rats, *J. Neurochem. 65*, 2290−2298.
30. Sheppard, C. W (1962) *Basic Principles of the Tracer Method: Introduction to Mathematical Tracer Kinetics*, Wiley, New York.
31. Gibaldi, M., and Perrier, D. (1982) *Pharmacokinetics*, 2nd ed., Dekker, New York.

32. Comar, C. L. (1955) *Radioisotopes in Biology and Agriculture: Principles and Practice,* McGraw-Hill, New York.
33. Tetzloff, S. U., and Bizzozero, O. A. (1998) Palmitoylation of proteolipid protein from rat brain myelin using endogenously generated 18O-fatty acids, *J. Biol. Chem. 273*, 279−285.
34. Loisel, T. P., Adam, L., Hebert, T. E., and Bouvier, M. (1996) Agonist stimulation increases the turnover rate of beta 2AR-bound palmitate and promotes receptor depalmitoylation, *Biochemistry 35*, 15923−15932.
35. Mouillac, B., Caron, M., Bonin, H., Dennis, M., and Bouvier, M. (1992) Agonist-modulated palmitoylation of beta 2-adrenergic receptor in Sf9 cells, *J. Biol. Chem. 267*, 21733−21737.

BI049176U